



10th International Conference on Solid State Chemistry, Pardubice, Czech Republic

Structure of SnF₂-SnO-P₂O₅ Glasses

James York-Winegar^a, Tristan Harper^{a,b}, Carrie Brennan^b,
Justin Oelgoetz^a, Andriy Kovalskiy^{a,1*}

^aAustin Peay State University, Department of Physics and Astronomy, 601 College Street, Clarksville TN 37044, USA

^bAustin Peay State University, Department of Chemistry, 601 College Street, Clarksville TN 37044, USA

Abstract

Low melting point glasses, specifically tin fluorophosphates, have recently received attention as a successful host matrix to rare earth metals to be used in photon conversion for solar cell applications. We have used high resolution X-ray photoelectron spectroscopy and Raman microscopy to investigate the structure of 50SnF₂-20SnO-30P₂O₅ glass. To compliment this experimental study density functional theory was used to predict Raman spectra. The O 1s X-ray photoelectron spectra indicate a high non-bridging to bridging oxygen ratio, a sign of relatively high durability needed for this glass to be applied to solar energy. The experimental results are in good agreement with theoretical calculations.

© 2013 The Authors. Published by Elsevier B.V. Open access under [CC BY-NC-ND license](http://creativecommons.org/licenses/by-nc-nd/4.0/).

Selection and/or peer-review under responsibility of the Organisation of the 10th International Conference on Solid State Chemistry.

Keywords: Glass; Tin fluorophosphate; Raman; XPS; DFT; Solar; SnF₂-SnO-P₂O₅

1. Introduction

Solar cells have relatively low efficiency because only a small portion of the total solar energy passing through the atmosphere can be absorbed. By an appropriate photon up and down-conversion the spectrum of absorbed light can be significantly extended. Glass structures doped with rare earths or organic dyes are one possible method for photon conversion. Low melting point glasses, specifically tin fluorophosphate glasses, have been shown to be promising hosts for the converters; however, durability of these materials is still in question. It was shown that one of the ways to obtain more chemically durable phosphate glasses can be the depletion of bridging oxygen, which is usually associated with hydrolysis [1]. This is why structural studies of tin fluorophosphate glasses are an important topic and are investigated in this work.

¹ * Corresponding author. Tel.: +1-931-221-6157; fax: +1-931-221-6129.
E-mail address: kovalskyya@apsu.edu.

The structure of these glasses has been previously studied using X-ray photoelectron spectroscopy (XPS) [2] and Raman spectroscopy methods [3,4]. Analysis of O 1s XPS core level spectra showed that for the $50\text{SnF}_2\text{-}20\text{SnO-}30\text{P}_2\text{O}_5$ composition the ratio of non-bridging to bridging oxygen is relatively high, leading to an increase in durability [2]. Raman spectroscopy studies have indicated the possibility for high chemical durability due to low signal associated with bridging oxygen modes [3,4].

The resolution of the methods previously used did not allow for the structural features to be established with sufficient precision. That is why the application of high resolution XPS in combination with Raman microscopy will provide us with the real bulk and surface structure of the low melting glasses needed for efficient application of these materials in solar energy. Density functional theory (DFT) was used to calculate electronic ground state geometries and to predict the Raman spectra of the glasses. DFT calculations have numerous advantages, including being computationally inexpensive compared to post Hartree-Fock methods such as n^{th} -order Møller–Plesset perturbation theory (MPn) and gives results that are complementary to experimental data. Raman spectra of glasses are difficult to simulate using quantum chemistry codes (such as in the present study) as the large random network is modeled by a relatively small portion of the network accounting for less random variations in the model structure than in the network. This causes the broad band Gaussians associated with vibrational modes in glasses to narrow, typically becoming a series of sharply peaked Lorentzians instead. As such, multiple representative structures need to be run in order to discern trends in the line positions and intensities.

2. Experimental

The studied glass samples have a composition of $50\text{SnF}_2\text{-}20\text{SnO-}30\text{P}_2\text{O}_5$, made from reagent grade components. Raw materials were mixed in an argon environment and melted in an air atmosphere at 250°C for 15-25 minutes in an alumina crucible. The melt was poured into a room temperature copper mould consisting of a ring covered with two plates. Samples were stored in a desiccator before measurement to prevent contamination.

High resolution XPS spectra were measured using an ESCA Scienta 300 spectrometer with monochromatic Al-K α X-rays as the excitation radiation. To examine the bulk structure the glasses were fractured in UHV 10^{-9} torr immediately before measurement. To avoid influence of surface charging on the recorded spectra, a flood gun of slow electrons was used for charge compensation.

Raman spectra were measured with a HORIBA XploRa confocal Raman microscope using a 532 nm excitation laser. The laser power was filtered by 75% to approximately 22 mW. The spectral resolution was maximized to 1 cm^{-1} using 1800 gratings, 100 μm wide slit, and 200 μm hole diameter. Samples were measured one day after quenching to prevent contamination. Raman spectra from the surface and the volume of the samples were measured.

DFT electronic ground state and Raman spectra calculations were used to complement the experimental data. Several initial geometries were created, based on high resolution XPS spectra. Hydrogen atoms were used to terminate strings of covalent bonds, allowing us to keep the structures moderate in size. Calculations were performed using Gaussian 09 revision B1 [5] (G09) using the B3LYP [6] exchange-correlation functional. In these calculations, the LANL08 [7-9] basis set was used for the Sn and P atoms and LANL2DZ [10-12] basis set for the F and O atoms.

3. Results

3.1 XPS Spectra

XPS is considered one of the fundamental structural methods for amorphous solids. Brow et al. [2] used this method to study the structure of $\text{SnF}_2\text{-SnO-P}_2\text{O}_5$ glasses of various compositions. Their results for the O 1s spectra of $50\text{SnF}_2\text{-}20\text{SnO-}30\text{P}_2\text{O}_5$ glass indicate a high ratio of non-bridging to bridging oxygen (19:1). However, it is known from a previous infrared spectroscopy study of the glass that 5-10% bridging oxygen atoms exist [13]. The F 1s spectra show that fluorine is present in both F-P and F-Sn sites with the majority connected to P. They also report an average Sn $3d_{5/2}$ binding energy of 487.9 ± 0.1 eV without specification of any fitting. The modern high resolution XPS technique allows us to verify these valuable data and obtain information for the core level spectra of other atoms in the system.

The analysis of O 1s core level spectrum of $50\text{SnF}_2\text{-}20\text{SnO-}30\text{P}_2\text{O}_5$ glass (Fig. 1a) confirms the previous conclusion on the minor concentration of bridging oxygen in the matrix. The peak contains two components centered at 531.7 eV (non-bridging oxygen) and 533.0 eV (bridging oxygen). According to our data 7.8% of oxygen atoms form the bridging P-O-P bonds. Such a high non-bridging to bridging oxygen ratio is usually considered as evidence for high chemical durability of glass which is required for solar energy applications.

It was possible to establish quite precisely the percentage of fluorine atoms in two different chemical environments, more specifically, bonded with P and Sn atoms whose components are situated at 687.23 eV and 684.7 eV, respectively (Fig. 1b). According to the calculations the ratio of F-Sn to F-P is 4:5. These results testify that both types of structural units play an important role in the formation of glass structure.

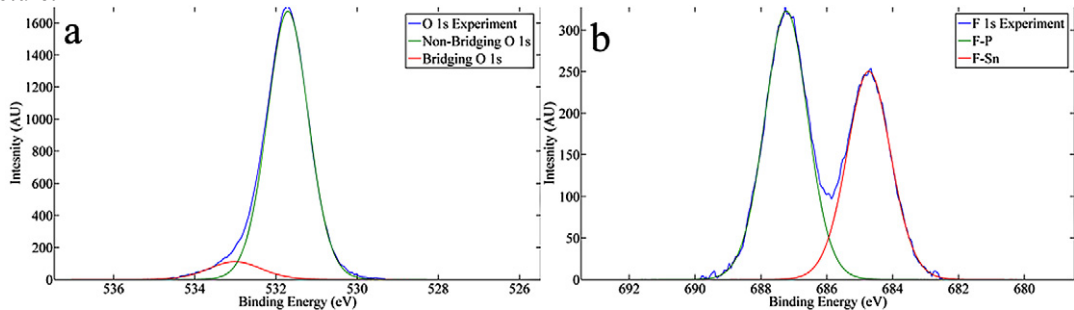


Fig. 1. (a) O 1s XPS spectra of $50\text{SnF}_2\text{-}20\text{SnO-}30\text{P}_2\text{O}_5$; (b) F 1s XPS spectra of $50\text{SnF}_2\text{-}20\text{SnO-}30\text{P}_2\text{O}_5$

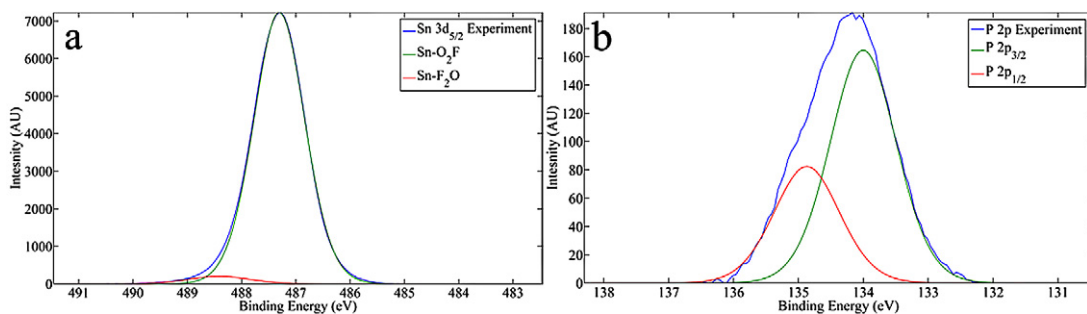


Fig. 2. (a) Sn $3d_{5/2}$ XPS spectra of $50\text{SnF}_2\text{-}20\text{SnO-}30\text{P}_2\text{O}_5$; (b) P 2p XPS spectra of $50\text{SnF}_2\text{-}20\text{SnO-}30\text{P}_2\text{O}_5$

It is clear from the analysis of previous two spectra that the Sn atoms should be bonded with oxygen as well as fluorine within Sn-O₂F and Sn-F₂O molecular blocks. The former is the preferable configuration in agreement with Brow et al. [2]. The Sn 3d_{5/2} core level spectra confirm this statement with the major component centered at 487.3 eV and the minor one at 488.4 eV (Fig. 2a). The P 2p core level spectrum contains two components which are associated with spin orbit splitting of the level and which represent only one chemical environment, namely P-O₃F. The P 2p_{3/2} component is located at 134.0 eV.

3.2 Raman Spectra

Analysis of previous Raman spectroscopy data for the structural units of interest allows us to list the major bands which can be expected in our spectra. The band near 250 cm⁻¹ was assigned to the Sn-O₂ bending vibration [14]. The band in the 500 cm⁻¹ region was associated with P-F bending modes [15]. In the 600 cm⁻¹ peak was connected with SnO₂-F structural units [16]. The 750 cm⁻¹ band was associated with P-F stretching modes [17]. The most interesting bands from the point of environmental durability are those between 650 cm⁻¹-775 cm⁻¹ which were linked to bridging oxygen (P-O-P) symmetric stretching modes and the 950 cm⁻¹ band associated with bridging oxygen asymmetric stretching modes [4,18,19].

The Raman spectra were measured both on the surface and inside the volume of the glass. The latter (Fig. 3a) contain nearly all previously described peaks with various intensities with the exception of those related to bridging oxygen (650 cm⁻¹-775 cm⁻¹ and 950 cm⁻¹). The absence of these peaks is in good agreement with O 1s XPS spectra of the bulk glass indicating a high ratio of non-bridging to bridging oxygen.

The surface Raman spectrum of the glass (Fig. 3b) reveals a major peak centered at 360 cm⁻¹ which possibly corresponds to the F-PO₃ scissoring mode which is supported by DFT Raman calculations described below. The surface also has a strong peak centered at 478 cm⁻¹ and a weak band at 590 cm⁻¹. The surface spectra of the glass shows no evidence of bridging oxygen usually associated with the 950 cm⁻¹ band [18]. Another peak which can be linked to the bridging oxygen at 700 cm⁻¹ [4,19] has very low intensity indicating a relatively environmentally durable surface structure. We can see that the structure of the surface layer is quite different from the structure of the bulk, but the thickness of the surface layer is still an open question.

It is known that Raman spectra calculated from DFT tend to overshoot experimental data with respect to wavenumbers [20]. The overestimation has been shown to be relatively uniform and the systematic error can be remedied by applying a constant scaling factor to the wavenumber axis [21,22]. Most scaling factor fits for DFT methods are computed for single functional and basis set combinations [21,22,23,24]. Since we used a combination of B3LYP with LANL08 and LANL2DZ the scaling factor is unknown at this time; however, most scaling factors for the B3LYP functional are approximately 0.97 [21,22,23,24], which accounts for the overshoot in our DFT calculations versus the experimental data. The theoretical Raman spectra of the glass (Fig. 3a, Fig. 3b) are used for peak identification and are not scaled by theoretical activity or scaling factors. Optimized geometries used to calculate Raman spectra are also given (Fig. 4) [2]. Figures of optimized geometry were processed in Avogadro [25].

DFT Raman spectra calculations of this glass correspond to the bulk structure of the glass and show good agreement with previous experimental Raman studies. This match is significant because it can provide information on bands that have not been previously assigned (or have not found satisfactory assignment in the literature search) such as the bands in the 350 cm⁻¹-450 cm⁻¹ region. The simulated Raman spectra show that there is a strong possibility that this region is associated with the F-PO₃ scissoring mode. The calculated Raman spectra from various initial geometries consistently indicate this

mode in a series of strong lines. There is also evidence for P-O stretching modes in the 750-900 cm^{-1} region. The large range of this mode at different chemical environments can be associated with the broad band centered at 877 cm^{-1} in the Raman spectra of the bulk glass.

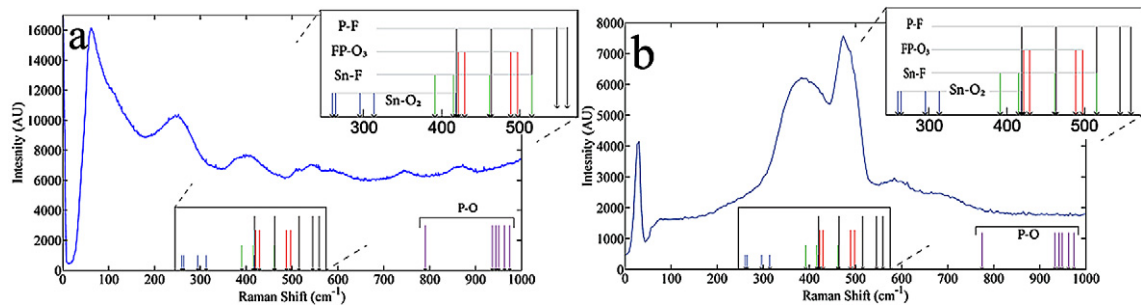


Fig. 3. (a) Raman spectrum of the freshly cut surface in the bulk of $50\text{SnF}_2\text{-}20\text{SnO-}30\text{P}_2\text{O}_5$ glass and calculated Raman spectra without wavenumber scaling, where height of theoretical Raman spectra corresponds to the source of a vibrational mode and not Raman intensity.; (b) Raman spectrum measured on the surface of $50\text{SnF}_2\text{-}20\text{SnO-}30\text{P}_2\text{O}_5$ glass and theoretical Raman spectra without wavenumber scaling, where height of theoretical Raman spectra corresponds to the source of a vibrational mode and not Raman intensity.

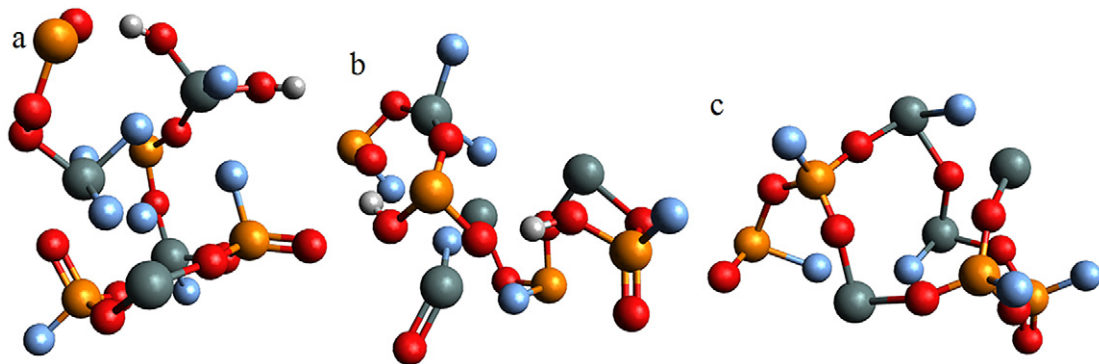


Fig. 4. Three optimized geometries for $50\text{SnF}_2\text{-}20\text{SnO-}30\text{P}_2\text{O}_5$ glass with initial conditions based off XPS data [2]. Orange atoms represent P, Dark Grey—Sn, red—O, light blue—F, and white—H. Hydrogen atoms, where present, were added to terminate the structures, and are not believed to be a present in the actual glass samples.

4. Conclusion

High resolution X-ray photoelectron spectroscopy, Raman microscopy, and density functional theory were used to characterize the structure of $50\text{SnF}_2\text{-}20\text{SnO-}30\text{P}_2\text{O}_5$ glass. The results from both experimental methods show quite good agreement with theoretical calculations. The bulk structure of the glass is characterized by the high ratio between non-bridging to bridging oxygen, occupation of fluorine in two different chemical states (F-P and F-Sn), two types of structural units which contain Sn (the preferred $\text{Sn-O}_2\text{F}$ and minor $\text{Sn-F}_2\text{O}$), and the single chemical environment for P atoms ($\text{P-O}_3\text{F}$ structural units). Such a structure has potential as a durable glass host for doping with rare earths and organic dyes for up and down conversion of solar radiation.

Acknowledgements

We would like to thank NSF's International Materials Institute New Functionality in Glass (NSF Grant No. DMR 0844014) and NASA Tennessee Space Grant Consortium for funding support. We would also like to thank Dr. Roman Golovchak (Lehigh University) for taking XPS measurements. Calculations were carried out on the Austin Peay Computing Cluster, which was funded by NSF MRI grant CNS 0722890. Raman spectra were measured using a HORIBA XploRA confocal Raman microscope which was funded by NASA grant NNX10AJ04G.

References

- [1] Tick PA. Water durable glasses with low melting temperatures. *Phys Chem Glasses* 1984; **25**(6), 149-54 .
- [2] Brow RK, Phifer CC, Xu XJ, Day DE. An XPS Study of Anion Bonding in Tin(II)-Fluorophosphate Glass. *Phys Chem Glasses* 1992; **33**[2], 33-9.
- [3] Xu XJ, Day DE. Structure of tin fluorophosphate glasses containing PbO or B₂O₃. *Phys Chem Glasses* 1995; **36**(6), 264-71.
- [4] Lim JW, Yung SW, Brow RK. Properties and structure of binary tin phosphate glasses. *J Non-Cryst Solids* 2011; **357**, 2690-4.
- [5] Frisch MJ, Trucks GW, Schlegel HB, Scuseria GE, Robb MA, Cheeseman JR, Scalmani G, Barone V, Mennucci B, Petersson GA, Nakatsuji H, Caricato M, Li X, Hratchian HP, Izmaylov AF, Bloino J, Zheng G, Sonnenberg JL, Hada M, Ehara M, Toyota K, Fukuda R, Hasegawa J, Ishida M, Nakajima T, Honda Y, Kitao O, Nakai H, Vreven T, Montgomery JA Jr, Peralta JE, Ogliaro F, Bearpark M, Heyd JJ, Brothers E, Kudin KN, Staroverov VN, Kobayashi R, Normand J, Raghavachari K, Rendell A, Burant JC, Iyengar SS, Tomasi J, Cossi M, Rega N, Millam JM, Klene M, Knox JE, Cross JB, Bakken V, Adamo C, Jaramillo J, Gomperts R, Stratmann RE, Yazyev O, Austin AJ, Cammi R, Pomelli C, Ochterski JW, Martin RL, Morokuma K, Zakrzewski VG, Voth GA, Salvador P, Dannenberg JJ, Dapprich S, Daniels AD, Farkas Ö, Foresman JB, Ortiz JV, Cioslowski J, Fox DJ. *Gaussian 09* Revision B.1 2012; Gaussian Inc.
- [6] Becke AD. Density-functional thermochemistry. V. systematic optimization of exchange-correlation functionals. *J Chem Phys*, 1997; **107**, 8554.
- [7] Roy LE, Hay PJ, Martin RL. Revised basis sets for the LANL effective core potential. *J Chem Theory Comput* 2008; **4**(7), 1029-31.
- [8] Hay PJ, Wadt WR. Ab initio effective core potentials for molecular calculations, Potentials for the transition metal atoms Sc to Hg. *J Chem Phys* 1985; **82**, 270-83
- [9] Wadt WR, Hay PJ. Ab initio effective core potentials for molecular calculations, Potentials for main group elements Na to Bi. *J Chem Phys* 1985; **82**, 284-98
- [10] Dunning Jr TH, Hay PJ. Methods of Electronic Structure Theory. *Mod Theor Chem* 1976; **3**, 1-28
- [11] Hay PJ, Wadt WR. Ab initio effective core potentials for molecular calculations, Potentials for K to Au including the outermost core orbitals. *J Chem Phys* 1985; **82**, 299-310
- [12] Dunning Jr. TH, Hay PJ. *Methods of Electronic Structure Theory: Vol. 2*. Ed: Schaefer HF. 3rd ed. Plenum Press; 1977
- [13] Xu XJ, Day DE. Properties and structure of Sn-O-P-F glasses. *Phys Chem Glasses* 1990; **31**(5), 183-7
- [14] McGuire K, Pan ZW, Wang ZL, Milkie D, Menéndez J, Rao AM. Raman studies of semiconducting oxide nanobelts. *J Nanosci Nanotechnol* 2002; **2**, 1-4
- [15] Shimonouchi T. Tables of molecular vibrational frequencies: Consolidated volume II. *J Phys Chem Ref Data* 1977; **6**, 993-1102
- [16] Nichev H, Sendova-Vassileva M, Andreev P, Dimova-Malinovska D, Starbova K. Preparation of wire structured ZnO films by electrochemical deposition. *J Phys Conf Ser* 2010; **16**, 1-5
- [17] Baran EJ, Weil M. Vibrational spectra of the layered monofluorophosphate (V), NH₄Ag₃(PO₃F)₂. *J Raman Spectrosc* 2009; **40**, 1698-1700
- [18] Fletcher LB, Witcher JJ, Reichman WB, Arai A, Bovatsek J, Kroll DM. Changes to the network structure of Er-Yb doped phosphate glass induced by femtosecond laser pulses. *J Appl Phys* 2009; **106**, 083107
- [19] Koudelka L, Klikorka J, Frumar M, Pisárčik M, Kellö V, Khalilev VD, Vakhrameev VI, Chkhenkeli GD. Raman spectra and structure of fluorophosphate glasses of (1-x)Ba(PO₃)₂-xLiRAIF₆. *J Non-Cryst Solids* 1986; **85**, 204-10
- [20] Hehre WJ, Radom L, Schleyer PvR, Pople J. A. *Ab Initio Molecular Orbital Theory*. Ed: 1st ed. Wiley; 1986
- [21] Andrade SG, Luísa CS, Gonçalves CS, Jorge FE. Scaling factors for fundamental vibrational frequencies and zero-point energies obtained from HF, MP2, and DFT/DZP and TZP harmonic frequencies. *J Mol Struct-Theochem* 2008; **864**, 20-5
- [22] Scott AP, Radom L. Harmonic Vibrational Frequencies: An Evaluation of Hartree-Fock, Møller-Plesset, Quadratic Configuration Interaction, Density Functional Theory, and Semiempirical Scale Factors. *J Phys Chem* 1996; **100**, 16502-13

[23] Sinha P, Boesch SE, Gu C, Wheeler RA, Wilson A. Harmonic Vibrational Frequencies: Scaling Factors for HF, B3LYP, and MP2 Methods in Combination with Correlation Consistent Basis Sets. *J Phys Chem A* 2004; **108**, 9213-17

[24] Palafox M. Scaling Factors for the Prediction of Vibrational Spectra. I. Benzene Molecule. *Int J Quantum Chem* 2000; **77**, 661-84

[25] Hanwell MD, Curtis DE, Lonie DC, Vandermeersch T, Zurek E, Hutchison GR Avogadro: An advanced semantic chemical editor, visualization, and analysis platform. *J Cheminf* 2012; **4**:17, 1-33